Approximate Analysis of Bridges for the Routing and Permitting Procedures of Overweight Vehicles

Attila Vigh[1] and László P. Kollár[2]

Abstract: The paper presents a method for comparing the mechanical effects of overweight and design load vehicles on bridges. There is no restriction on the arrangement of the axles and on the size of the axle loads. The bridge may be a simple span bridge, a continuous girder, a truss girder, or an arch. Even for a very complex bridge structure the only required parameter of the bridge is the span length. The presented method is a robust and reliable tool for the permitting process of overweight vehicles, which is verified by several thousand comparisons.

DOI: 10.1061/(ASCE)1084-0702(2006)11:3(282)

CE Database subject headings: Approximation methods; Bridges; Bridge loads; Routing; Permits; Vehicles.

Introduction

Overweight and oversize vehicles require permits to reach their destination. To obtain the optimum route an optimization process (Osegueda et al. 1999; Adams et al. 2002) must be developed which includes the evaluation of the load bearing capacities of the bridges and the verification of geometrical constraints along the route (Osegueda et al. 1999). In this paper, we focus only on the analysis of bridges.

Bridges are designed according to design guides and standards, which prescribe the safety factors and the design load.

When a bridge is evaluated for an overweight vehicle, the designer may choose from the following options: (1) he or she may perform a detailed structural analysis, similarly as it is done for the design load; or (2) he or she may apply a simplified structural analysis, such as a comparison of the internal forces (bending moment, shear force, normal force) resulting from the design load and overweight vehicle. Usually both of these procedures are time consuming and require several data of the bridge. In many cases, simplified methods are feasible, which are based on (3) the comparison of the axle loads. One of the best-known methods is the application of the "federal bridge formula" (*Bridge Formula Weights* 1994), which also has several improvements (James et al. 1986; Chou et al. 1999; Kurt 2000).

In this paper, a new method is presented that can be used for arbitrary design load/overweight vehicle combinations and for any kind of bridge structures.

Problem Statement

We consider a bridge of the highway system, which can be a simple span bridge, a continuous girder, a truss girder, or an arch bridge (Fig. 1). The bridge has been designed for a load defined in the national standard [Fig. 2(a)]; this load will be referred to as "design load vehicle" (DLV). The bridge is subjected to a vehicle load that has arbitrary axle spacings and axle loads. This vehicle requires a permit. It is referred to as an "overweight vehicle" (OV). Examples of DLV and OV are shown in Fig. 2. We wish to determine the stress ratio for the bridge, defined as

$$n = \min\left(\frac{E^{\mathrm{DLV}}}{E^{\mathrm{OV}}}\right) \tag{1}$$

where E denotes a relevant effect on the bridge, such as bending moment, normal force, shear force, punching shear at any section of the bridge, or the reaction forces resulting from the vehicle load. The superscripts DLV and OV refer to the design load

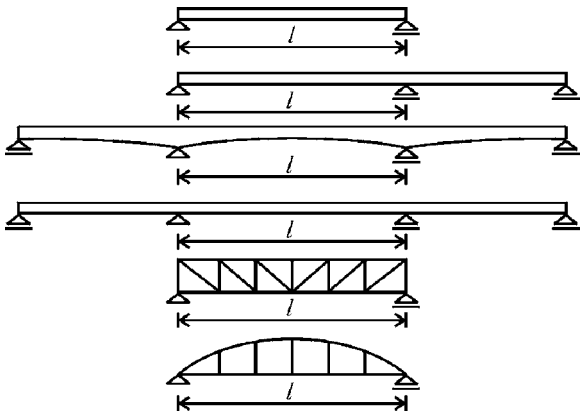

Fig. 1. Bridge structures

[1]Research Fellow, Hungarian Academy of Sciences, Research Group of Engineering Structures, Budapest Univ. of Technology and Economics, Dept. of Mechanics, Materials, and Structures, Müegyetem rkp. 1-3, Budapest, H-1521 Hungary. E-mail: vigh@silver.szt.bme.hu

[2]Professor, Budapest Univ. of Technology and Economics, Dept. of Mechanics, Materials, and Structures, Müegyetem rkp. 1-3, Budapest, H-1521 Hungary. E-mail: lkollar@eik.bme.hu

Note. Discussion open until October 1, 2006. Separate discussions must be submitted for individual papers. To extend the closing date by one month, a written request must be filed with the ASCE Managing Editor. The manuscript for this paper was submitted for review and possible publication on December 1, 2004; approved on April 12, 2005. This paper is part of the ***Journal of Bridge Engineering***, Vol. 11, No. 3, May 1, 2006. ©ASCE, ISSN 1084-0702/2006/3-282–292/$25.00.

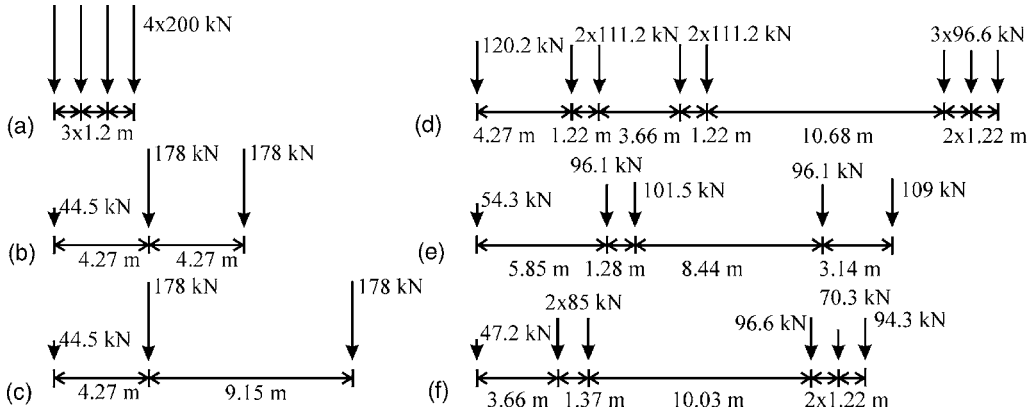

Fig. 2. Design load vehicles (a–c); overweight vehicles (d–f) (permit required)

vehicle and to the overweight vehicle, respectively. E^{DLV}/E^{OV} can be calculated for a large number of effects; however, we choose one that results in a smaller number, n.

If the safety level of the bridge designed for the DLV and the bridge subjected to the OV is the same, n is a measure of the safety of the bridge; when n is bigger than one, the OV may go across the bridge. In the analysis, we assume that the widths of the DLV and the OV are identical [a modification for taking into account the difference in the widths of the vehicles is given in Kollár (2001)]. [When the safety level is different for the original design and for the present calculation—for example, when overstrength factors are taken into account—a modification is needed that takes into account the live load/dead load ratio (James et al. 1986).

The distributed design load is not considered in this article. Note, however, that heavier, overweight vehicles may go across a bridge if the other vehicles are not permitted.

Approach

As we stated in the previous section the effects (e.g., the internal forces) caused by the DLV and by the OV must be determined, and their ratio, n, must be calculated. As an example, the bending moment envelopes of these loads are calculated on a simply supported girder [Fig. 3(a)]. When the maximum bending moments are compared, n is equal to

$$n = \frac{M_{\max}^{DLV}}{M_{\max}^{OV}}$$

The internal forces can also be determined with the aid of influence lines. This is illustrated for the bending moment of the midspan cross section in Fig. 3(b). The bending moments calculated by the loading of the structure and by the loading of the influence line are identical. Every relevant effect (internal forces, reaction forces) must be calculated and compared, and consequently, every relevant influence line must be considered. Typical influence lines for different bridge structures are shown in Fig. 4.

We observe that only the shapes of the influence lines are important—their ordinates are irrelevant because we are interested only in the ratio (n) and not in the real values of the internal forces.

Here we propose the usage of three artificial influence lines, shown in Fig. 5. The maximum ordinates of these lines are chosen as shown in Fig. 5; however, as we stated above, these values do not influence the results of the calculations. The lengths of the influence lines (x) varies between zero and a maximum value (e.g., the length of a simply supported bridge, $0 \leqslant x \leqslant l$); the maximum value will be discussed for different bridges in the verification section. For a simply supported beam η_M and η_B are identical to the shape of the reaction force influence line and to the bending moment influence line of the midsection, respectively, when $x=l$. For a continuous span bridge, the influence

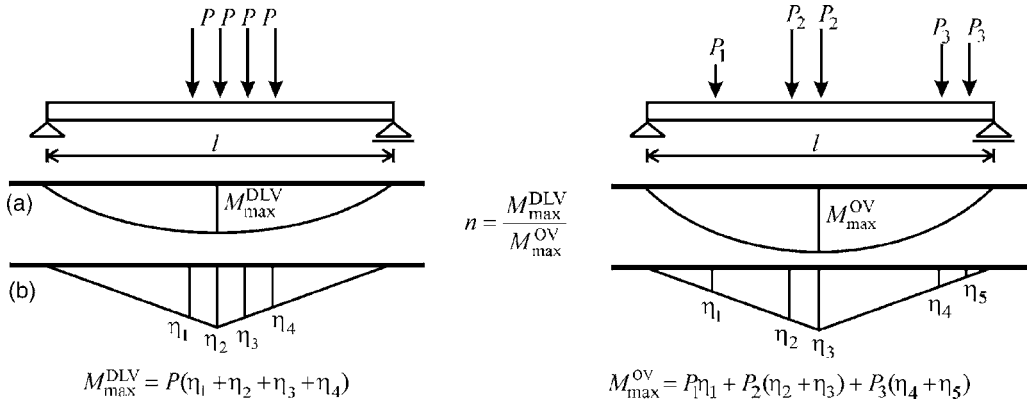

Fig. 3. (a) Bending moment envelopes of a simple span bridge subjected to the DLV and to the OV and (b) calculation of the midspan bending moment with the aid of the influence line

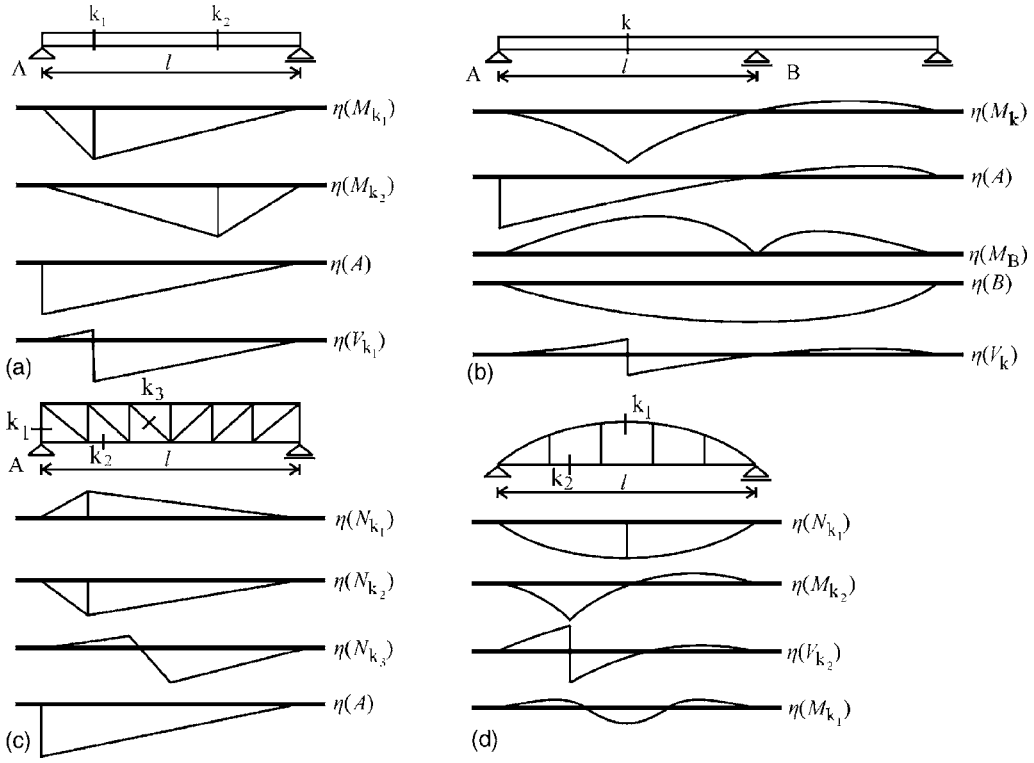

Fig. 4. Typical influence lines of bridge structures: M, A (or B), V, and N refer to the bending moment, reaction force, shear force, and normal force, respectively

lines are curved and the lines given in Fig. 5 can be considered as the approximations of the "accurate" influence lines.

The application of these three artificial influence lines has several advantages over the accurate calculation of the internal forces: (1) most importantly, it requires very few input data—in addition to the axle spacing and axle loads, only the spans of the bridges are needed; and (2) the calculation is very fast (the required algorithm is given in Appendix III).

We recall that the method of comparison of the axle loads also has the above advantages over the accurate calculation. Hence the question arises: why do we need a new method? The usage of the artificial influence lines has the advantage over the comparison of the axle loads that it is more accurate and more robust. It was demonstrated by several researchers that the comparison of the axle loads (e.g., the use of the federal bridge formula) may be inaccurate, should be used only for limited spans (James et al. 1986) and gross loads, and only for simple span bridges. (The comparison of the three methods is also shown in Table 1.)

We must admit that the proposed method has a few disadvantages: it is less accurate than the accurate calculation of the internal forces, and may result in either a too conservative or an unsafe design. This question will be addressed in the verification section, and we will see that the proposed method has reasonable accuracy. A disadvantage of the method of artificial influence lines over the comparison of the axle loads is that it is more complicated—the latter requires the application of a simple formula, which can be used also with hand calculation. We must agree with this criticism; however, we emphasize that (1) the same number of inputs are needed in both methods (the comparison of axle loads also requires the knowledge of the bridge span, because it may be used only under a maximum span); and (2) the calculation of the artificial influence lines can be carried out by very fast matrix manipulations (loops can be avoided). These calculations require a computer, but the method is fast and reliable (see Appendix III).

The usage of the artificial influence lines is demonstrated in Fig. 6. The right column can be interpreted as the comparison of the midspan bending moments of a simple span bridge. $M^{\mathrm{DLV}}(x)$=the maximum value obtained from η_B (with length x) considering every possible position of the DLV. M^{OV} is calculated similarly. The strength ratio is defined as

$$n_B = \frac{E_B^{\mathrm{DLV}}}{E_B^{\mathrm{OV}}} = \frac{M^{\mathrm{DLV}}}{M^{\mathrm{OV}}} \tag{2}$$

It can be seen that the bending moment induced by the DLV is greater than that of the OV when x is smaller then 6 m; however, it is smaller when $x>6$ m. The middle column can be considered the comparison of either the reaction forces or the maximum shear forces, while the left column can be considered the

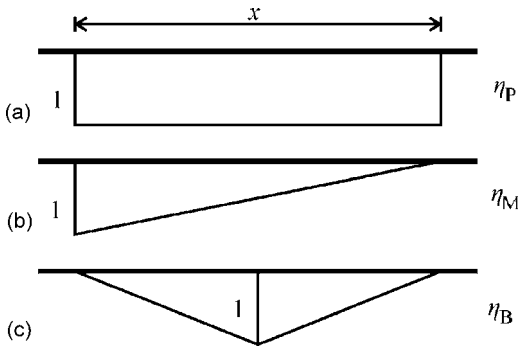

Fig. 5. Proposed "artificial" influence lines

Table 1. Comparison of Present Method with Accurate Calculation of Internal Forces and with Comparison of Axle Loads

Type	Accurate calculation of internal forces	Comparison of axle loads	Artificial influence line (present)
Accuracy	High	Poor or limited application	Acceptable
Required input data	Hundreds or thousands	Axle loads and spacing+spans	Axle loads and spacing+spans
Required analysis	Complex (computer)	Simple formula (hand calculation)	Few matrix calculations (computer)

comparison of the maximum total load of the vehicles over a distance x.

Failure of the Main Girders and of the Second-Order Members

The bridge is a complex structure that may consist of main girders, cross girders, bridge deck, etc., and we must avoid the failure of any of them. Failure of the main girder or of the supports is referred to as "global failure," while the failure of the cross girders, bridge deck, etc., is called "local failure."

The local failure of the bridge deck can be caused by the punching shear induced by one axle, which can be investigated by the comparison of the maximum axle loads. This is identical to the usage of η_P [Fig. 6(a)] with $x=0$. The punching can also be caused by two axles that are close to each other. For example, in Fig. 6 the two axles of the OV are closer to each other than the axles of the DLV, but the resultant of these two axles is still smaller than the maximum axle load of the DLV. This is shown in the left column of Fig. 6, where at $x=2$ m, $E_P=178$ and 170 kN for the DLV and OV, respectively. As a consequence η_P can be used to investigate the local failure, where x should be significantly smaller than the span of the bridge (for example, $0 \leqslant x \leqslant 0.2l$). The load on the cross girder depends on the locations and the stiffnesses of the girders. The influence lines of these girders can have different shapes—their (positive) parts are significantly shorter than the span. We propose to use all the three artificial influence lines to take into account the local effects. The stress ratio for local effects is defined as

$$n^{\text{loc}} = \min(n_P, n_B, n_M), \quad 0 \leqslant x \leqslant l^{\text{loc}} \tag{3}$$

where l^{loc}=short distance (e.g., $l^{\text{loc}}=0.2l$).

When we compare the internal forces of the main girder due to the DLV and due to the OV, we may face the following problem, which is illustrated in Fig. 7 for a simply supported single span bridge. The dashed line is the bending moment envelope due to the DLV, while the solid line is the bending moment envelope due to the OV. It can be seen that the midsection can carry the OV: $M^{\text{DLV}} > M^{\text{OV}}$. However, close to the support, where the bending

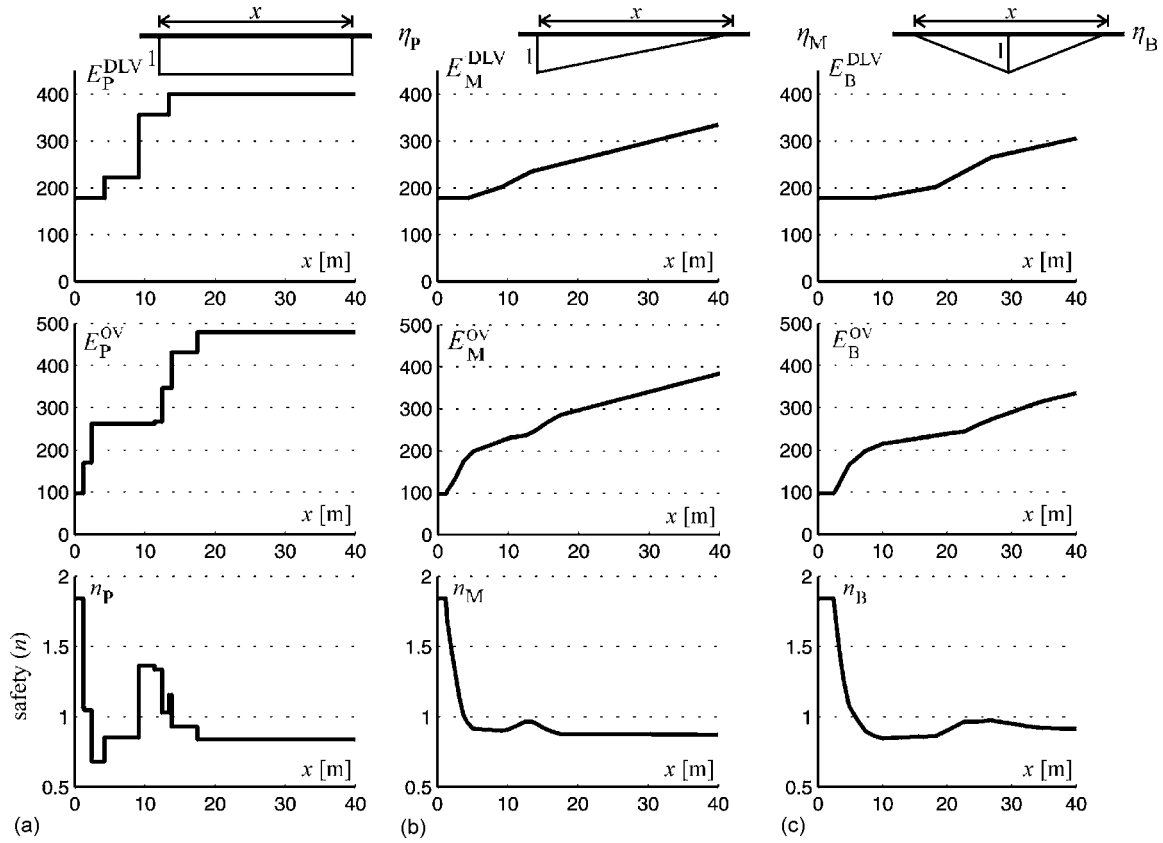

Fig. 6. Resultants according to the three influence lines subjected to the DLV shown in Fig. 2(c) and to the OV shown in Fig. 2(f); results are presented as functions of the length of the influence lines

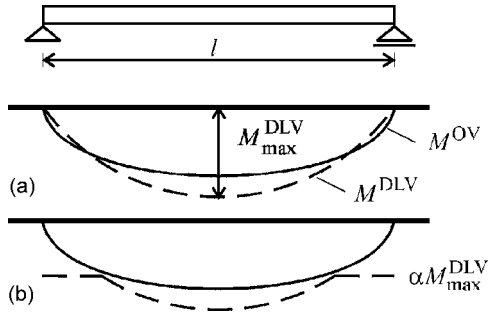

Fig. 7. (a) Bending moment envelopes and (b) modification of the envelope due to the DLV

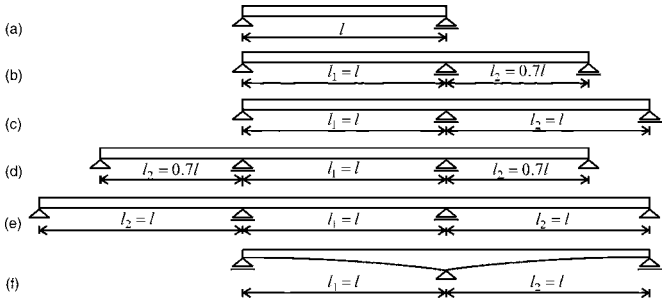

Fig. 8. Simple span and multispan bridges considered in the verifications

moments are small, $M^{DLV} < M^{OV}$. As a consequence, when the bridge cross sections are designed exactly for M^{DLV}, it cannot carry the OV. In reality, cross sections with internal forces less than the maximum value are built to larger dimensions and therefore have a higher safety level. In addition, in practical design, the sections have minimum dimensions and as a consequence a minimum load-bearing capacity. Hence a parameter α is introduced, and it is assumed that every cross section is capable to carry at least αM_{max} bending moment. By so doing the bridge shown in Fig. 7(b) may carry the OV.

Verification

In this section, we will apply the method of artificial influence lines for simple span bridges, two span bridges, continuous span bridges, trusses, and arches, and we will determine the accuracy of the suggested method. The accurate calculation was carried out with a finite-element program containing beam elements.

First, we have calculated the maximum internal forces (and maximum reactions) caused by the DLV. They are denoted by $\hat{E}_i^{DLV}$ $(i=1\ldots I)$, where I=total number of the investigated forces along the bridge. When $\hat{E}_i^{DLV}$ is smaller than αE_{max}^{DLV} [where $E_{max}^{DLV}=\max(\hat{E}_i^{DLV})$], it is replaced by αE_{max}^{DLV}; hence we write $E_i^{DLV}=\max(\hat{E}_i^{DLV}, \alpha E_{max}^{DLV})$.

Then, we calculate the internal forces (and maximum reactions) induced by the OV, which are denoted by E_i^{OV}. The accurate stress ratio of the bridge is defined as

$$n^{accurate} = \min\left(\frac{E_i^{DLV}}{E_i^{OV}}, n^{loc}\right) \tag{4}$$

where n^{loc}=stress ratio [Eq. (3)] according to the local failure.

Next, n_P, n_M, and n_B are calculated as described in the approach section, and the stress ratio is calculated by

$$n = \min(n_P, n_M, n_B) \tag{5}$$

where n_P, n_M, and n_B are calculated for different lengths

$$n_P: 0 \le x \le l_P; \quad n_M: 0 \le x \le l_M; \quad n_b: 0 \le x \le l_B \tag{6}$$

The accuracy of the method can be determined by

$$\beta = \frac{n^{accurate}}{n} \tag{7}$$

When $\beta=1$, the result is accurate; when $\beta>1$ the method is conservative; and when $\beta<1$ it is not conservative.

In Fig. 2, some of the vehicle loads are shown that are considered in the verification. In Figs. 2(a–c) the Hungarian and the U.S. DLV are given (*Standard Specifications* 1989). Figs. 2(d–f) show real truck loads. Note that in the verification of the method the gross weights of the vehicles do not matter. In Appendix II we list all the vehicle loads that were taken into account in the verification.

We have calculated the β parameter, and the smallest and the highest values of β are given in tables of the following subsections. The results depend on the following parameters:

- Type and geometry of the bridge;
- Type of DLV [we will consider three cases: the DLV is given in Fig. 2(a), denoted by "Hungary"; the DLV is given in Figs. 2(b and c), denoted by "USA"; and the DLV can be any of the loads listed in Tables 7 and 8, denoted by "ALL"];
- Parameter α, which is shown in Fig. 7;
- Distance l^{loc}, considered in the calculation of n^{loc}; and
- Distance l_P, l_M, l_B, considered in the calculation of n.

In the calculation, every single load in Tables 7 and 9 is taken into account as OV.

We emphasize that these comparisons (verifications) show the effect of global failure of the bridge. For those DLVs where the local failure governs the design [when Eq. (4) gives $n^{accurate}=n^{loc}$], β is obviously greater than or equal to unity. (In these cases the method may be more conservative than the values given in the following tables. A better accuracy can be achieved if we have knowledge on the details of the bridge.)

Simple Span Bridges

We consider a simple span bridge shown in Fig. 8(a). In the accurate calculation [Eq. (1)] we compared the bending moments, the shear forces, and the reaction forces. We considered five different spans, where l=10, 15, 20, 30, and 50 m.

The number of vehicle loads is 33; hence a total number of 2,860 bridge calculations were carried out. (The bending moment and shear force envelope were, in each case, calculated by loading the bridge in more then 40 different positions.) The results are shown in Table 2. In the calculation of βs the following parameters were used: $l^{loc}=0.2l$, $l_B=l_M=l$.

Note that in this case η_M and η_B give the exact shear force at the support and the exact bending moment at the midspan.

Continuous Span Bridges

We considered two-span and three-span bridges shown in Figs. 8(b–f), with spans l=10, 15, 20, 30, and 50 m. In the accurate calculation we take into account the bending moments, shear

Table 2. Accuracy of Method (β_{min}/β_{max}) for Simply Supported Bridges as a Function of l_P and α

l_P	DLV	$\alpha=0.5$	$\alpha=0.7$	$\alpha=0.9$	$\alpha=1.0$
$0.2l$	USA	0.96/1.19	0.96/1.19	0.96/1.19	0.96/1.22
	Hungary	0.98/1.03	0.98/1.03	0.98/1.03	0.98/1.03
	ALL	0.88/1.19	0.96/1.19	0.96/1.19	0.96/1.22
$0.6l$	USA	1.00/1.33	1.00/1.33	1.00/1.33	1.00/1.35
	Hungary	0.99/1.32	0.99/1.33	0.99/1.33	0.99/1.33
	ALL	0.90/1.66	0.96/1.66	0.97/1.66	0.98/1.66
$0.7l$	USA	1.00/1.33	1.00/1.33	1.00/1.33	1.00/1.35
	Hungary	1.00/1.42	1.00/1.42	1.00/1.42	1.00/1.42
	ALL	0.90/1.66	0.96/1.66	0.98/1.66	0.99/1.66
$0.8l$	USA	1.00/1.48	1.00/1.48	1.00/1.48	1.00/1.50
	Hungary	1.00/1.51	1.00/1.51	1.00/1.51	1.00/1.51
	ALL	0.90/1.66	0.96/1.66	0.98/1.66	0.99/1.66
l	USA	1.00/1.64	1.00/1.64	1.00/1.64	1.00/1.67
	Hungary	1.00/1.82	1.00/1.82	1.00/1.82	1.00/1.82
	ALL	0.90/1.95	0.96/1.95	0.98/1.95	0.99/1.95

Note: See Figs. 5(a) and 7.

forces, and the reaction forces. In the calculation of βs $l^{loc}=0.2l$, $l_B=l_M=l$ were considered. The results for $l_P=l_1+0.6l_2$ and $\alpha=0.5$ are given in the top three rows of Table 3. The last three rows were calculated similarly to those of Table 5, which will be discussed in the section on arch bridges. Further results are presented in Vigh (2006).

For the last case [Fig. 8(f)] it was assumed that the second moment of inertia is changing from I_0 to $8I_0$, following a second order parabola.

Truss Bridges

We consider trusses with the shapes shown in Fig. 9. The numbers of cells were 6, 12, 18, 24, and 30, while the lengths were 10, 20, 30, 40, and 50 m. In the accurate calculation we calculate the bar forces and reaction forces. The total number of the calculated cases was about 5,720. The results are given in Table 4; further results can be found in Vigh (2006).

Arch Bridges

We consider the arch bridges with the geometrical and stiffness characteristics shown in Fig. 10. The height of the arch was

Table 3. Accuracy of Method (β_{min}/β_{max}) for Multispan Bridges

DLV	Fig. 8(b)	Fig. 8(c)	Fig. 8(d)	Fig. 8(e)	Fig. 8(f)
(a) Every axle					
USA	0.89/1.45	0.88/1.49	0.85/1.41	0.85/1.46	0.88/1.49
Hungary	1.00/1.47	1.00/1.26	0.98/1.38	0.98/1.40	1.00/1.26
ALL	0.89/1.49	0.88/1.49	0.85/1.41	0.80/1.51	0.88/1.49
(b) Axles that increase the effect					
USA	0.89/1.45	0.88/1.50	0.85/1.44	0.85/1.48	0.88/1.50
Hungary	1.00/1.47	1.00/1.26	0.98/1.38	0.98/1.40	1.00/1.26
ALL	0.89/1.49	0.88/1.50	0.85/1.44	0.85/1.51	0.88/1.50

Note: $l_P=l_1+0.6l_2$ and $\alpha=0.5$.

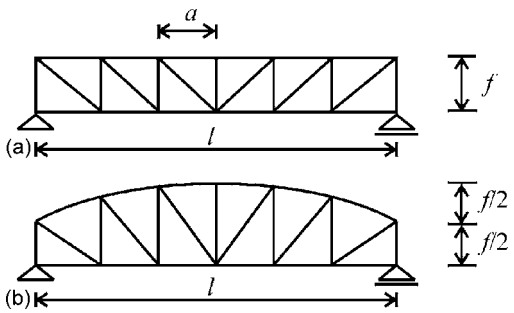

Fig. 9. Truss bridges considered in the verifications

$f=0.3l$, the axial elongation of the columns were neglected, and it was assumed that their connections to the arch and to the deck are hinged. The spans of the bridge are $l=20$, 30, 40, and 50 m, while the number of suspenders are $n5,15$. In the accurate analysis we calculated the axial forces in all the elements, the bending moments and the shear forces in the arch and in the deck, and the reaction forces. The results are given in the upper three rows of Table 5.

The accuracy of the calculation is significantly smaller than in the previous cases. The reason is that the influence lines of the deck consist of both positive and negative parts, while the artificial influence lines have only positive parts. The change in sign within an influence line means that some of the axles may reduce the total effect of the vehicle load. Engineering practice often does not take into account these axles, and for example, according to the Eurocode [European Standard EN1991-2 (European Standard 2002)], the designer must neglect those axles, which reduce the effect (moment, stress, etc.) at the considered cross section. The accurate calculations were also carried out with this assumption: we took into account—for the DLV—only those axles that increase the effect at a given cross section. The results of the calculation are presented in the lower three rows of Table 5.

Numerical Example

We consider a two-span bridge, both with 10-m spans [Fig. 11(a)]. The bridge was designed for the DLV with three axles [Fig. 2(c)], and its gross weight is 400.5 kN. The OV has six axles [Fig. 2(f)], and its gross weight is 478.4 kN.

We wish to calculate the safety (n) of the bridge with the approximate method of artificial influence lines and also to determine the accuracy of the method with the aid of the calculation of internal forces.

Table 4. Accuracy of Method (β_{min}/β_{max}) for Truss Bridges

DLV	Fig. 9(a)	Fig. 9(b)
USA	1.00/1.94	1.00/1.94
Hungary	1.00/1.43	1.00/1.43
ALL	0.99/2.13	0.99/2.13

Note: $l_P=0.2l$ and $\alpha=0.5$.

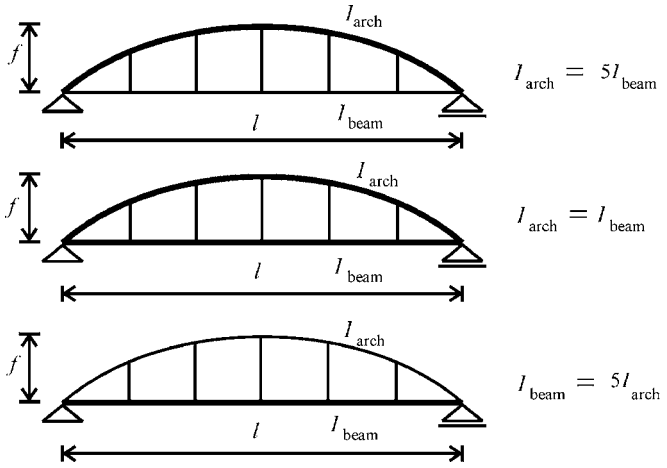

Fig. 10. Arch bridges considered in the verifications (I=second moment of inertia)

First, we calculate the internal forces and maximum reaction forces caused by the DLV and OV numerically. The shear force and bending moment envelopes are shown in Figs. 11(b and c). We may expect that the critical section of a two-span bridge be either at the midspans or at the middle support. In this case, the critical cross section is left of the middle span [identified by a bullet in Fig. 11(c)]; here, the ratio of bending moments is the lowest, with $n^{\text{accurate}}=M^{\text{DLV}}/M^{\text{OV}}=0.802$. Both the shear force ($V^{\text{DLV}}$) and the bending moment (M^{DLV}) envelopes caused by DLV contain a horizontal line due to a minimum load bearing capacity. As we mentioned before, every cross section can carry at least $\alpha T_{\max}$ shear force and $\alpha M_{\max}$ bending moment, where $\alpha=0.5$.

Then, we use the artificial influence lines. The effects E_P, E_M, and E_B caused by the DLV and the OV are shown in Fig. 6. The safety, defined as $n=E^{\text{DLV}}/E^{\text{OV}}$ is also shown in Fig. 6, and it is reiterated in Fig. 12(a). In Fig. 12(b), the minimum values of n in the $0\ldots x$ interval are plotted. As it was stated in the continuous span bridge section, the P line is evaluated at $l_P=l_1+0.6l_2$ (here $l_1=l_2=l=10$ m), while the M and the B lines are evaluated at $l_B=l_M=l$; thus we have $n_P=0.682$ at $l_P=16$ m and $n_M=0.890$, $n_B=0.860$ at $l_B=10$ m.

Finally, the minimum safety is calculated as $n=\min(n_P,n_M,n_B)=n_P=0.682$. The comparison of internal forces gave 0.802. We found that in this case, the approximate calculation is on the safe side, and the difference is only 18%.

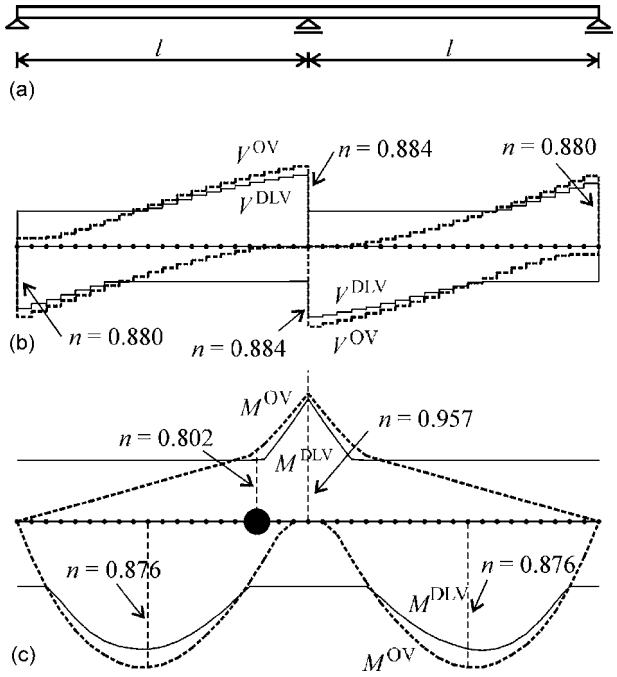

Fig. 11. Geometry of: (a) two-span bridge; (b) shear force; and (c) bending moment envelopes ($n=V^{\text{DLV}}/V^{\text{OV}}$ or $n=M^{\text{DLV}}/M^{\text{OV}}$)

Discussion

In this paper we presented a new method for comparing the effects of overweight and design load vehicles. This method contains a few parameters listed in the verification section. In the calculations, for every type of bridge, the maximum length of l_M and l_B was equal to the span of the bridge (or to the longest span of a multispan bridge). The reason is that these are good approximations of the shear force and bending moment influence lines. The length of l_P was chosen according to the result of the numerical calculations, which are summarized in Table 6.

The α value was also investigated numerically, and it was found that $\alpha=0.5$ can be recommended for every case.

Table 5. Accuracy of Method ($\beta_{\min}/\beta_{\max}$) for Arch Bridges

DLV	$I_{arch}=5I_{beam}$	$I_{arch}=I_{beam}$	$I_{beam}=5I_{arch}$
(a) Every axle			
USA	0.73/1.51	0.95/1.66	0.96/1.71
Hungary	0.86/1.42	0.98/1.43	1.00/1.45
ALL	0.73/1.80	0.87/1.80	0.88/1.80
(b) Axles that increase the effect			
USA	0.95/1.51	0.97/1.66	0.97/1.71
Hungary	0.87/1.42	0.98/1.43	1.00/1.45
ALL	0.87/1.82	0.95/1.80	0.96/1.80

Note: See Fig. 10; $l_P=0.7l$ and $\alpha=0.5$.

Table 6. Accuracy of New Method ($\beta_{\min}/\beta_{\max}$) for Different Bridges

	Bridge structure			
DLV	Simple span	Multispan	Truss	Arch
USA	0.96/1.19	0.85/1.50	1.00/1.94	0.95/1.71
Hungary	0.98/1.03	0.98/1.47	1.00/1.43	0.87/1.45
ALL	0.88/1.19	0.85/1.51	0.99/2.13	0.87/1.82
l_P	$0.2l$	$l_1+0.6l_2$	$0.2l$	$0.7l$

Note: The recommended and applied parameters are $l_B=l_M=l$, and l_P is given in the last row. In the calculation, we took into account all the loads given in Tables 7 and 8 as OV, while the considered DLVs are as follows: for USA, the load is given in Figs. 2(b and c); for Hungary, the load is given in Fig. 2(a); and for ALL, all the loads are considered, which are given in Tables 7 and 9.

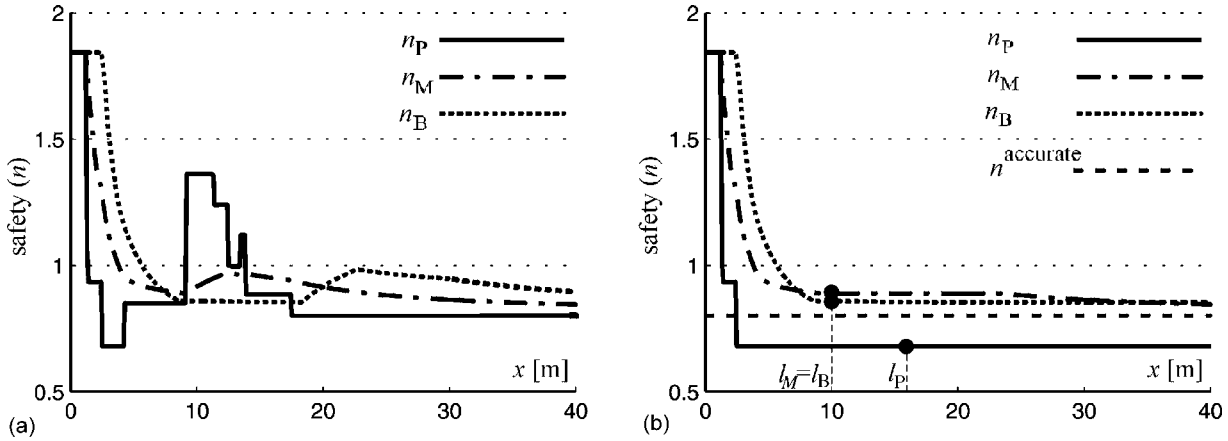

Fig. 12. (a) Safeties n_P, n_M, n_B due to the P, M, and B influence lines as the function of length and (b) minimum values of n_P, n_M, and n_B in the $0 \ldots x$ interval ($n^{\text{accurate}}=0.8$ is calculated with the comparison of the internal forces)

With these parameters more than 15,000 calculations were carried out to verify the method. In most of the cases, the method is conservative; the maximum error on the unsafe side is 15%, as summarized in Table 6 for different bridge structures (the error on the unsafe side can also be compensated by applying a safety factor).

The main advantage of the method is that it requires very little bridge data (the spans), and it is robust and reliable, which is demonstrated and verified by several thousand comparisons.

This method can serve as the basic building block of the permitting procedure of overweight vehicles. In an application, it is worthwhile to extend the method by considering the effect of (1) the distributed loads and (2) the effect of the width of the load and the position of the load perpendicular to the bridge axis.

The presented method, together with the listed parameters, was built in a computer program, which is used by the Technical and Information Services on National Roads, Hungary.

In developing the method, after the birth of the basic idea (Kollár 2001) we were facing the questions: Which and how many artificial influence lines have to be taken into account (possibly different lines for different bridge structures), to obtain a robust, reliable, and relatively simple procedure?

For example, we may consider only the η_P influence lines (with a total length of $l_P=l$ for simple span) instead of the three lines given in Fig. 5(a). As a result the accuracy is significantly less—on the unsafe side it is about 0.9, while on the safe side it is very high (as can be seen, for example, in simply supported bridges in Table 2, last line). As a consequence, the application of η_P only is not recommended.

To apply a few further influence lines may increase the $\beta_{\min}$ value; however, it also may increase the $\beta_{\max}$ values, and hence it is not recommended either. It can also be shown (see Appendix III) that influence lines with arbitrary shapes may give very conservative results.

A possible change in the method is to use a trapezoidal line instead of η_P to avoid "jumps" in the $E(x)$ lines. It was found (Vigh 2006) that it has only very minor effects on the accuracy of the method and it is more complicated than the method described in Appendix III.

Our recommendation, as it was stated before, is to use the lines in Fig. 5, with the parameters given in Table 6.

Acknowledgment

This work was supported by the Ministry of Economy and Transport, Hungary (GVOP-3.1.1-2004–05–0141/3.0), which is highly appreciated.

Appendix I. Determination of the "Most Dangerous" Influence Lines

As stated in the approach section, the different effects (such as bending moment, shear force, etc.) can be investigated with the aid of influence lines. We suggested three artificial influence lines given in Fig. 5. The question arises: Can we determine mathematically those influence lines that give the lowest value of n? By so doing, we may have a process, which is conservative and scientifically rigorously proven.

It is easy to show in an example that this process may lead to a result that is too conservative and cannot be used in the practical cases. Let us consider a DLV and an OV with identical axle loads, but different axle spacing. The minimum value of n is resulting

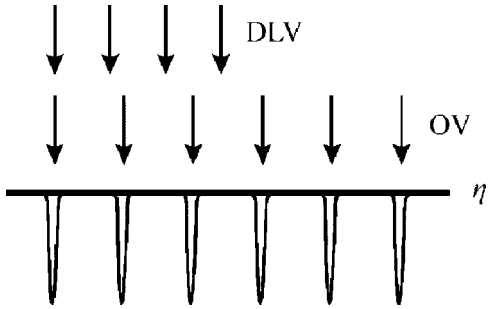

Fig. 13. Unrealistic influence line

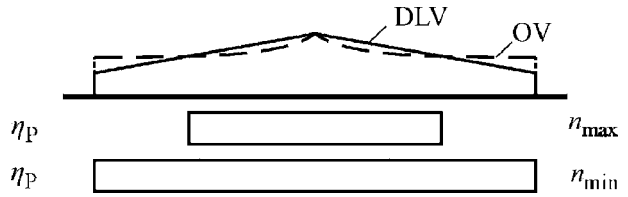

Fig. 14. Two influence lines that result in the lowest and the highest value of n when the loads are symmetrical and continuous with one intersection point

from the influence line, which has zero values everywhere, but under the axles of the OV, it is equal to unity (Fig. 13). For this case $n=1/m$, where m=number of axles of the OV. Note that this influence line results in a mathematical minimum; however, it is unrealistic and gives unreasonable results. (This is the reason why we investigated "real" structures in the verification section.)

Let us now investigate a problem that has limited practical use but is closer to the real cases. Let us assume that both the DLV and the OV are symmetrical continuous loads, which are monotonously increasing from the left to the middle. We also assume that the yet unknown influence line has the same characteristics. For simplicity, we assume that the maximum value of the DLV and OV are the same as shown in Figs. 14 and 15. For the case when there is one intersection of the function OV and DLV (Fig. 14) it can be shown that the influence lines result in the lowest and the highest n when the influence lines are uniform [denoted by η_P in Fig. 5(a)]. When the functions of the loads have more intersections the influence lines that provide the maximum and minimum n must be chosen from those constant influence lines, which end at the intersection points. As can be seen from this example, the η_P line can serve as the "most dangerous" influence line in many cases.

When the loads are not symmetrical and they are not monotonic, more complex influence lines may be the most dangerous. In Fig. 16, we show two examples where for the given OV and DLV, we determined numerically the influence lines, which result in the lowest n. Note that we applied the restriction to the influence lines that they are positive and must have a monotonically increasing and a monotonically decreasing part. In the calculation, the "fmins" algorithm of MATLAB was used. The influence lines were composed with 20 linear sections, hence the optimization included 21 parameters.

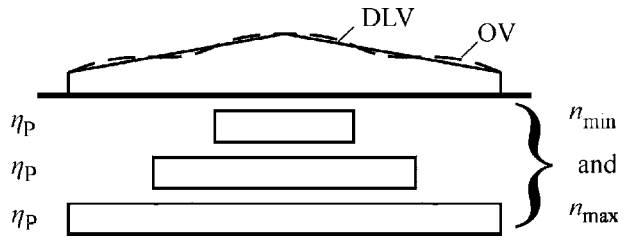

Fig. 15. Three influence lines that result in the lowest and the highest value of n when the loads are symmetrical and continuous with many intersection points

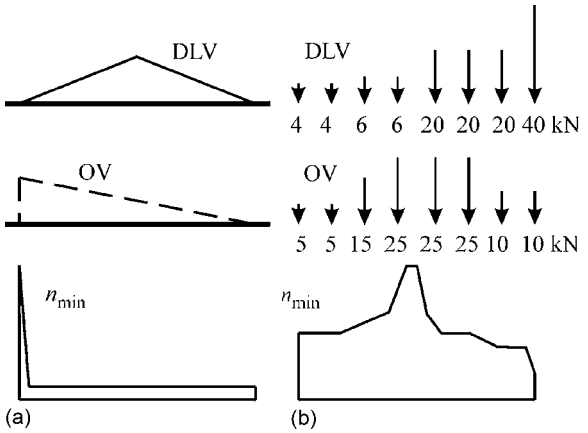

Fig. 16. Examples of the "most dangerous" influence lines: (a) $n=0.73$ ($n_P=0.98$, $n_M=0.91$, and $n_B=1$) and (b) $n=2.32$ ($n_P=2.50$, $n_M=2.88$, and $n_B=2.46$)

Appendix II. Considered Vehicle Loads

Table 7. Axle Load and Axle Spacing of the Artificial DLVs and OVs

	DLV and OV (artificial vehicles)			
Number	Axle load	Axle spacings [m]	Gross weight [kN]	Overall length [m]
1		0.2		4
2	21 axles	0.4		8
3	101...101 kN	0.6		12
4		0.8		16
5		1.0		20
6		0.2		4
7	21 axles	0.4		8
8	201...1 kN	0.6	2,121	12
9		0.8		16
10		1.0		20
11		0.2		4
12	21 axles	0.4		8
13	1...201...1 kN	0.6		12
14		0.8		16
15		1.0		20

Table 8. Axle Load and Axle Spacing of Real DLVs

Number	Axle load [kN]	Axle spacings [m]	Gross weight [kN]	Overall length [m]
116	200–200–200–200	1.2–1.2–1.2	800.0	3.60
117	35.6–142.4	4.27	178.0	4.27
118	35.6–142.4–142.4	4.27–4.27	320.4	8.54
119	35.6–142.4–142.4	4.27–9.15	320.4	13.42
120	44.5–178–178	4.27–4.27	400.5	8.54
121	44.5–178–178	4.27–9.15	400.5	13.42
122	106.8–106.8	1.22	213.6	1.22

Table 9. Axle Load and Axle Spacing of Real OVs

Number	Axle load [kN]	Axle spacings [m]	Gross weight [kN]	Overall length [m]
216	120.2–111.2–111.2–111.2–96.6–96.6–96.6	4.27–1.22–3.66–1.22–10.68–1.22–1.22	854.8	23.49
217	104.1–118.8–116.1	4.88–1.4	339.0	6.28
218	70.8–69.4–118.8–113.5	2.93–1.46–1.62	372.5	6.01
219	48.1–99.7–127.3–129.1	4.33–5.91–1.19	404.2	11.43
220	54.3–96.1–101.5–96.1–109	5.85–1.28–8.44–3.14	457.0	18.71
221	47.2–95.2–95.2–96.6–70.3–94.3	3.66–1.37–10.03–1.22–1.22	498.8	17.50
222	40.1–103.2–84.1–87.2–74.8	3.87–7.01–3.14–6.86	389.4	20.88
223	44.1–45.4–47.2–56.5–66.8–61.4	5.27–1.49–6.46–3.02–7.22	321.4	23.46
224	56.1–58.7–97–100.1–74.3–80.1–76.1–79.7	4.69–1.4–1.55–11.80–1.74–1.55–4.85	622.1	27.58
225	53.4–89–89–89–89–89–89–89–89	4.4–1.4–4.3–1.4–11.9–1.4–4.3–1.4	765.4	30.50
226	51.2–56.3–56.3–66.5–66.5–66.5–66.5–66.5	4.27–1.22–7.32–2.44–7.32–2.44–7.32	496.3	32.33

Appendix III. Calculation of the Effects with the Artificial Influence Lines

The most dangerous placement of loads on a structure (or on an influence line) can be determined by moving the load in small steps along the structure (or along the influence line). This calculation must be carried out, in our case, for different lengths of the influence lines, which requires a step-by-step increase of the length of the lines. To avoid this time-consuming calculation, a simple, very fast algorithm is presented below. The calculation, instead of a double loop, requires matrix manipulations only.

Calculation of E_P

We consider a vehicle load that consists of n concentrated (axle) loads (Fig. 17, top). There are $n(n+1)/2$ different possible arrangements of loads, which are shown also in Fig. 17 and explained below.

The very left force, which is placed on the influence line, can be $P_1, P_2, \ldots, P_{n-1}, P_n$ as shown in the rows of Fig. 17. The last load is denoted by P_k and k can take the values shown in Fig. 17, on the right. As we stated above, there are $m=n+(n-1)+(n-2)+\ldots+1=n(n+1)/2$ arrangements. We treat these force arrangements as load cases, from $t=1$ to m; in every case we have a force vector (e.g., $\mathbf{P}_i=\{P_j, P_{j+1}, \ldots, P_k\}$) and a distance vector ($\mathbf{d}_i$, the elements of $\mathbf{d}_i$=distances of the forces from the first (left) force, hence the first element is zero), and we also determine the length of the load (l_i), the distance between the first and last force. In Fig. 17, $l_i=l_{jk}$ is shown.

The effect E_P can be calculated for every load case. For example, for the ith load case, when the length of the influence line l is equal to or greater than the length of the load case (l_i), $X_{P,i}$ is the sum of the forces

$$E_{P,i} = \mathbf{P}_i \mathbf{e}_i \text{ if } l \geq l_i$$

where $\mathbf{e}_i$=vector containing unities and it has the same number of elements as $\mathbf{P}_i$. The $E_{P,i}, l_i$ values are shown in Fig. 18(a). $E_{P,i}$ is valid for any value of $l \geq l_i$. In this calculation every possible load case is considered, and hence we can make the envelope, as shown in Fig. 18(b), obtain the $E_P(l)$ curve.

Calculation of E_M

The load cases are identical to those which were determined for the calculation of $E_{P,i}$. The loads may move backward, which we take into account by considering two η_M lines, as shown in Fig. 19 (and the directions of the loads will not be changed).

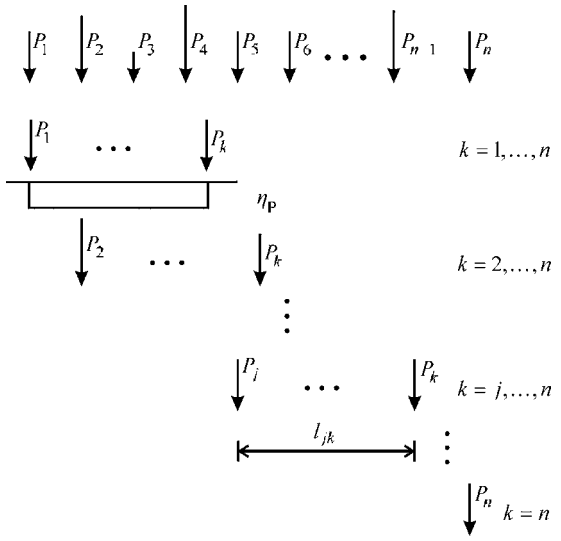

Fig. 17. Calculation of the P line

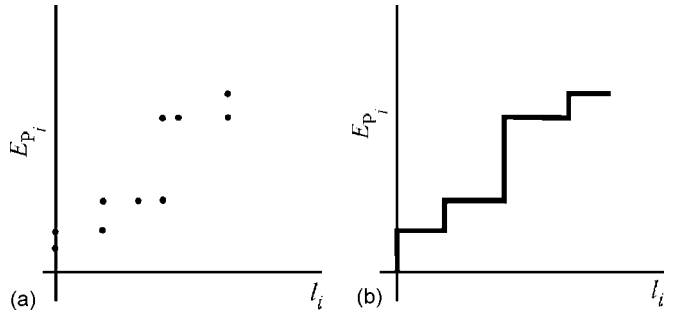

Fig. 18. Determination of $E_P(l)$ curve

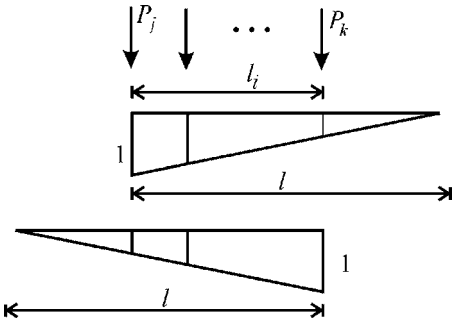

Fig. 19. Calculation of the M line

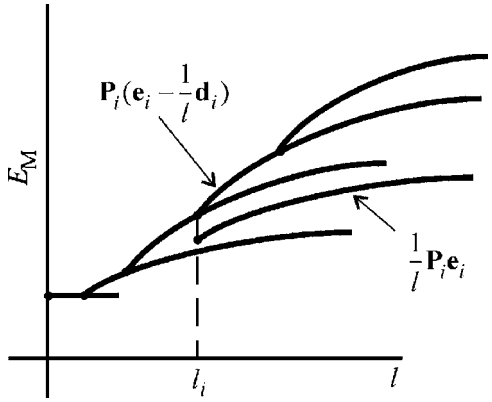

Fig. 20. Determination of $E_M(l)$ curve

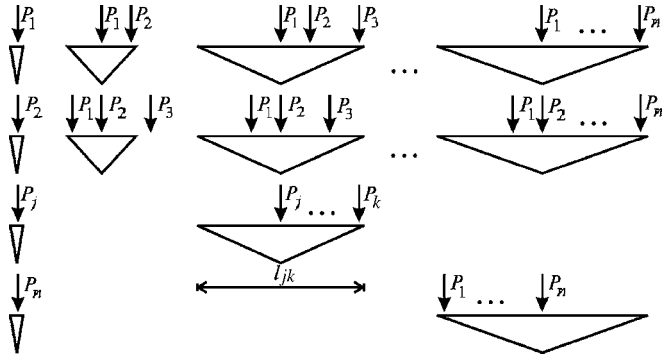

Fig. 21. Calculation of the B line

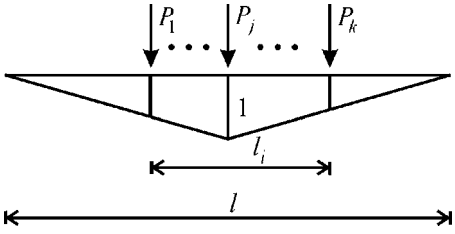

Fig. 22. Determination of $E_B(l)$

For the ith load case (Fig. 19), when the peak of the triangle is on the left

$$E_{M,i}^{l_i} = \mathbf{P}_i\left(\mathbf{e}_i - \frac{1}{l}\mathbf{d}_i\right) \quad \text{if } l \geqslant l_i$$

while when the peak is on the right

$$E_{M,i}^{l_i} = \frac{1}{l_i}\mathbf{P}_i\mathbf{e}_i \quad \text{if } l \geqslant l_i$$

which is shown in Fig. 20.

Calculation of E_B

When the influence line is a symmetrical triangle, one of the forces must be placed at the peak of the triangle. Accordingly, either P_1 or $P_2, \ldots,$ or P_n must be placed at the peak, as shown in the rows of Fig. 21.

In every row there are n different load arrangements; hence we consider a total number of load cases $m=n^2$.

The length of the ith ($i=1,2,\ldots,m$) load case $l_i=l_{jk}$ is twice the distance between the jth and the kth force. For each case a distance vector $\mathbf{d}_i$ and a force vector $\mathbf{P}_i$ is obtained. The elements of $\mathbf{d}_i$ are the distances of the forces from the force placed at the peak of the triangle ($\mathbf{P}_j$). The effect $E_{B,i}$ can be calculated as (Fig. 22)

$$E_{B,i} = \mathbf{P}_i\left(\mathbf{e}_i - \frac{2}{l}|\mathbf{d}_i|\right) \quad \text{if } l \geqslant l_i$$

where $|\mathbf{d}_i|$=vector, the elements of which are equal to the absolute values of the elements of $\mathbf{d}_i$.

Using the above expression we can determine the envelope of E_B as was done for E_M.

References

Adams, T. M., Malaikrisanachalee, S., Blazquez, C., Lueck, S., and Vonderohe, A. (2002). "Enterprise-wide data integration and analysis for oversize/overweight permitting." *J. Comput. Civ. Eng.*, 16(1), 11–22.

Bridge formula weights. (1994). United States Department of Transportation, Federal Highway Administration, Washington, D.C.

Chou, K. C., Deatherage, J. H., Leatherwood, T. D., and Khayat, A. J. (1999). "Innovative method for evaluating overweight vehicle permits." *J. Bridge Eng.*, 4(3), 221–227.

European Standard *EN1991-2*. (2002). *Eurocode 1—Traffic loads on bridges*, European Committee for Standardization, Brussels.

James, R. W., Noel, J. S., Furr, H. L., and Bonilla, F. E. (1986). "Proposed new truck weight limit formula." *J. Struct. Eng.*, 112(7), 1589–1604.

Kollar, L. P. (2001). "Load bearing capacities of bridges for overweight vehicles." *Közl. és Mélyépítéstud. Szemle.*, 51(9), 349–356 (in Hungarian).

Kurt, C., E. (2000). "A proposed modification of the bridge gross weight formula." *Proc., Mid-Continent Transportation Symp.*, 104–108.

Osegueda, R., et al. (1999). "GIS-based network routing procedures for overweight and oversize vehicles." *J. Transp. Eng.*, 125(4), 324–331.

Standard specifications for highway bridges. (1989). 14th Ed., AASHTO, Washington, D.C.

Vigh, A. (2006). "Approximate calculation of bridges for routing and permitting of overweight vehicles." Ph.D. thesis, Budapest Univ. of Technology and Economics, Dept. of Mechanics, Materials, and Structures, Budapest, Hungary (in Hungarian).